

structure analysis presents a general problem, in particular if further charged lattice components of the relevant compound (small amounts of cations as well as anions located in cavities and channels) and large amounts of crystal water molecules cannot be clearly located, for instance due to disorder. In these cases, the formula including the charge can in principle only be determined if analytical data and the (formal) charges of all ingredients are taken into account. The analytical data, however, cannot be very accurate as firstly, the concentration of the mentioned charged lattice components is generally very small (but not the number of ions in the formula unit) and secondly, the large crystal water content varies to some extent. The isolated compound with cluster **1**, for instance, shows in addition to  $\text{NH}_4^+$  ions, an "uptake" of small amounts of  $\text{Na}^+$  and  $\text{Cl}^-$  ions which complicate the determination of the cluster charge by elemental analysis as the difference in the number of cations and anions is of relevance here. The real charge of **1** is smaller as mentioned earlier, namely 14 – which is in agreement with the average BVS (bond valence sum) values of 5.60 for the 70 (**1**) and 80 (**2**) molybdenum centers located in the peripheral incomplete double cubes, which are built up from four Mo atoms of the  $\{\text{Mo}_8\}$  units as well as one  $\{\text{Mo}_1\}$ -type center and six oxygen atoms. Each of the double-cube compartments contains two 4d electrons. Remarkably, the absolute divergence of the BVS values for the 56 (**1**) or 64 (**2**) outer peripheral ring positions from the  $\{\text{Mo}_8\}$  units is only  $\pm 0.05$  and for the 14 (**1**) or 16 (**2**) equatorial positions ( $\{\text{Mo}_1\}$ -type centers) only  $\pm 0.10$  for six different cluster structures. This corresponds (formally) to the 28 (for **1**) and 32 (for **2**)  $\text{Mo}^{\text{V}}$  centers and is (for the  $\{\text{Mo}_8\}$  part) also in agreement with the conclusions from the EHMO calculations and the redox titrations. A related problem in charge determination was also stressed by Pope and coworkers in an important publication,<sup>[3]</sup> though the determination of the charge of their particular cluster anion—as was also pointed out—is not so difficult. This is due to the fact that the oxidation states of the metal centers are clearly known.

- [13] The IR spectra of large clusters (of the type  $\{\text{Mo}_{36}\}$ ,<sup>[6]</sup>  $\{\text{Mo}_{57}\}$ ,<sup>[6]</sup> and partly  $\{\text{Mo}_{154}\}$ <sup>[1a-c]</sup>) can be modeled by superposition of (weakly coupled) characteristic vibrations of different  $\{\text{Mo}_m\text{O}\}$  fragments.<sup>[14b]</sup> This simplifies of course the proof of functional groups on the one hand, but on the other complicates the differentiation of species with different numbers of these fragments, as in the case of **1** and **2**.
- [14] A. Müller, J. Meyer, E. Krickemeyer, E. Diemann, *Angew. Chem.* **1996**, *108*, 1296–1299; *Angew. Chem. Int. Ed. Engl.* **1996**, *35*, 1206–1208; b) A. Müller, M. Ohm, H. Bögge, unpublished results.
- [15] A. Müller, E. Diemann, B. Hollmann, H. Ratajczak, *Naturwissenschaften* **1996**, *83*, 321–322.
- [16] The pinacoidal plates contain in the crystal lattice the smaller tetradecameric ring-type clusters corresponding to **1** with a 1:1 ratio of rings of composition  $[\{\text{Mo}_{21}\}_{14}\{\text{Mo}_8\}_{14}\{\text{Mo}_1\}_{14}]$  and  $[\{\text{Mo}_{21}\}_{13}\{\text{Mo}_8\}_{14}\{\text{Mo}_1\}_{14}]$ ; the latter have a defect. Structural data: space group  $\text{P}\bar{1}$ ;  $a = 31.007(2)$ ,  $b = 32.818(2)$ ,  $c = 47.325(3)$  Å;  $\alpha = 90.59(1)$ ,  $\beta = 90.11(1)$ ,  $\gamma = 96.70(1)^\circ$ ;  $V = 47826$  Å<sup>3</sup>;  $Z = 2$ ;  $R = 0.110$  for 57819 independent reflections ( $F_o > 4\sigma(F_o)$ ). The rhombic plates contain in the crystal lattice the larger  $\{\text{Mo}_{176}\}$ -type rings as in **2** but with different packing and with a substantially higher amount of crystal water molecules (ca. 600  $\text{H}_2\text{O}$ ). Structural data: space group  $\text{P}2_1/\text{n}$ ;  $a = 29.205(2)$ ,  $b = 64.040(4)$ ,  $c = 74.622(3)$  Å;  $\beta = 99.81(1)$ ;  $V = 137522$  Å<sup>3</sup>;  $Z = 4$ ;  $R = 0.192$  for 63952 independent reflections ( $F_o > 4\sigma(F_o)$ ).
- [17] Note added in proof: The resulting product mixture obtained here is still relatively complex, but this must be put into perspective against the background that generations of chemists have attempted in vain to isolate crystals from solutions of molybdenum blue type species. The investigation of these products is also complicated due to the fact that the lattice energy is very low resulting in a series of isolated compounds with different packing of the clusters. We have succeeded in developing synthetic methods in which crystalline substances can be isolated in a few days without amorphous coprecipitation. This synthesis refers to the mentioned cluster of the type  $\{\text{Mo}_{154}\}$  ( $R = 0.057!$ ) and  $\{\text{Mo}_{176}\}$ , which have  $\text{MeOH}$  ligands as well as  $\text{H}_2\text{O}$  ligands. (A. Müller, M. J. Koop, H. Bögge, M. Schmidtman, *Chem. Commun.* submitted; A. Müller, E. Krickemeyer, M. J. Koop, S. Q. N. Shah, H. Bögge, M. Schmidtman, *Z. Anorg. Allg. Chem.* submitted.)

## Expression of Chirality by Achiral Coadsorbed Molecules in Chiral Monolayers Observed by STM\*\*

Steven De Feyter, Petrus C. M. Grim, Markus Rücker, Peter Vanoppen, Christian Meiners, Michel Sieffert, Suresh Valiyaveetil, Klaus Müllen, and Frans C. De Schryver\*

Pasteur discovered almost 150 years ago the three-dimensional separation of the sodium ammonium salt of racemic tartaric acid in enantiomorphous crystals.<sup>[1]</sup> Since then, chemists have been intrigued by the concept of chirality. The development of the scanning probe techniques, such as scanning tunneling microscopy (STM)<sup>[2]</sup> and atomic force microscopy (AFM),<sup>[3]</sup> made it possible to locally probe monolayers. Only a few reports have dealt with the direct observation of supramolecular chirality in two dimensions by use of scanning probe techniques. Spontaneous breaking of chiral symmetry by achiral molecules in a Langmuir–Blodgett (LB) film was determined by Viswanathan et al. with AFM.<sup>[4]</sup> Enantiomorphous monolayer domains from achiral liquid crystalline molecules,<sup>[5]</sup> achiral purine molecules,<sup>[6]</sup> and didodecylbenzene molecules<sup>[7]</sup> on graphite have been observed by STM. Eckardt et al. reported the separation of chiral phases in monolayer crystals of racemic amphiphiles in LB films by AFM.<sup>[8]</sup> The direct observation of enantiomorphous monolayer crystals from liquid crystalline enantiomers and the formation of coexisting enantiomorphous domains from a racemate by STM have been described by Stevens et al.<sup>[9]</sup> Spontaneous resolution in two dimensions was recently demonstrated by grazing-angle X-ray diffraction.<sup>[10]</sup>

We have used small chiral organic molecules with hydrogen-bonding potential to self-assemble chiral physisorbed monolayers on a graphite surface. The *S* enantiomer of the chiral isophthalic acid derivative 5-[10-(2-methylbutoxy)-decyloxy]isophthalic acid (ISA, Figure 1A) was dissolved in 1-heptanol, and a small droplet was applied to the freshly cleaved surface of highly oriented pyrolytic graphite (HOPG). Figure 1B shows a STM image of the resulting monomolecular layer of (*S*)-ISA adsorbed to the basal plane of HOPG. The image reveals a closely packed arrangement of molecules on the graphite surface with submolecular resolution. The aromatic isophthalic acid head groups of (*S*)-ISA molecules can clearly be recognized as bright spots. Bright and dark refers to the black/white contrast in the images;

[\*] Prof. Dr. F. C. De Schryver, Dr. S. De Feyter, Dr. P. C. M. Grim, Dr. M. Rücker, P. Vanoppen  
Department of Chemistry, Laboratory of Molecular Dynamics and Spectroscopy  
Katholieke Universiteit Leuven  
Celestijnenlaan 200-F, BE-3001 Heverlee (Belgium)  
Fax: (+32)16-327989  
E-mail: frans.deschryver@chem.kuleuven.ac.be  
C. Meiners, M. Sieffert, Dr. S. Valiyaveetil, Prof. Dr. K. Müllen  
Max-Planck-Institut für Polymerforschung, Mainz (Germany)

[\*\*] The authors thank FWO and DWTC for continuing financial support through IUAP-IV-11. S.D.F. is a predoctoral fellow of the Fonds voor Wetenschappelijk Onderzoek. P.V. thanks the IWT for a predoctoral scholarship.

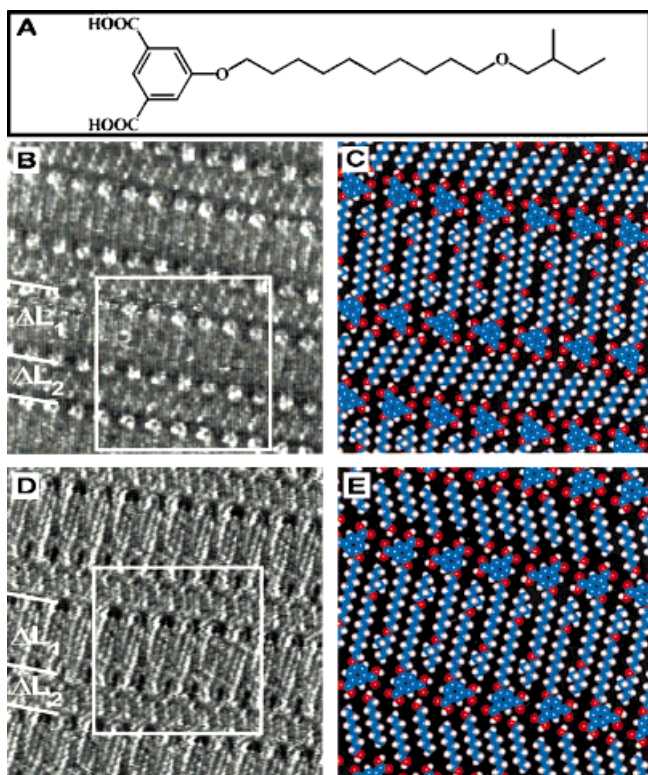


Figure 1. A) Chemical structure of ISA. B) STM image of an ordered monolayer of (*S*)-ISA molecules formed by physisorption at the 1-heptanol/graphite interface; image size:  $11.7 \times 11.7 \text{ nm}^2$ .  $\Delta L_1$  is the width of one lamella of interdigitated (*S*)-ISA molecules. The lamellar axis makes an angle  $\theta$  of  $+3.5 \pm 0.7^\circ$  with the normal to that graphite axis which is in alignment with the alkoxy chains (positive domain).  $\Delta L_2$  corresponds to the width of a lamella built up by 1-heptanol molecules. The solvent molecules form an angle  $\varphi$  of  $+20 \pm 3^\circ$  with the normal to the lamellar axis. C) Proposed molecular model for the two-dimensional packing of (*S*)-ISA molecules in the area shown in the STM image in B. D) STM image of an ordered monolayer of (*R*)-ISA molecules formed by physisorption at the 1-heptanol/graphite interface; image size:  $11.5 \times 11.5 \text{ nm}^2$ .  $\Delta L_1$  is the width of one lamella of interdigitated molecules. The lamellar axis makes an angle  $\theta$  of  $-3.8 \pm 0.6^\circ$  with the normal to that graphite axis which is in alignment with the alkoxy chains (negative domain).  $\Delta L_2$  corresponds to the width of a lamella built up by 1-heptanol molecules. The solvent molecules form an angle  $\varphi$  of  $-18 \pm 3^\circ$  with the normal to the lamellar axis. E) Proposed molecular model for the two-dimensional packing of (*R*)-ISA molecules in the area shown in the STM image in D.

white corresponds to the highest and black to the lowest measured tunneling current. Two different spacings are found between adjacent rows of (*S*)-ISA head groups. The largest spacing ( $\Delta L_1 = 30 \pm 1 \text{ \AA}$ ) corresponds to the dimension of the (*S*)-ISA molecules, and 1-heptanol molecules occupy the smaller space ( $\Delta L_2 = 10 \pm 1 \text{ \AA}$ ) between two rows of (*S*)-ISA head groups. The 1-heptanol molecules are coadsorbed and stabilized by the formation of hydrogen bonds with the (*S*)-ISA head groups. A similar observation was described by Vanoppen et al. for the imaging of achiral alkoxy-substituted isophthalic acid molecules dissolved in solvents such as 1-octanol or 1-undecanol.<sup>[11]</sup> Grim et al. also observed this codeposition of solvent molecules for a diacetylene-containing isophthalic acid derivative,<sup>[12]</sup> which then can be photopolymerized on the graphite surface.

To further analyze the structure of the monomolecular adlayer, a comparison with the underlying graphite surface is

made. Immediately after imaging an adlayer, the graphite surface underneath is visualized by lowering the bias voltage. This analysis indicates that the alkoxy groups are parallel to the graphite substrate and aligned with a graphite axis. The (*S*)-ISA molecules are interdigitated over the full length of the alkoxy groups. The stereogenic centers are not atomically resolved. The lamellar width indicates that the alkoxy chains tend to lie flat on the graphite surface to maximize the adsorption energy. Therefore, we suggest that the methyl group on the stereogenic carbon atom is pointing away from the graphite surface. The coadsorbed solvent molecules are not in alignment with a graphite axis. In this image, the angle  $\varphi$  between the solvent molecules and an imaginary line perpendicular to a row of (*S*)-ISA head groups is  $20 \pm 3^\circ$ . On the basis of the observed monolayer structure, a model for the molecular arrangement is proposed (Figure 1 C). The intra-lamellar distance between two head groups measures  $9.60 \pm 0.05 \text{ \AA}$ .

Comparison of the direction of the lamellar axes (any line parallel to a row of (*S*)-ISA head groups) with the underlying graphite substrate shows that the lamellar axis makes an angle  $\theta$  of  $+3.5 \pm 0.7^\circ$  with the normal to that graphite axis which is in alignment with the alkoxy chains. We call these domains positive/negative if a positive/negative<sup>[13]</sup> angle  $\theta$  is observed, irrespective of the orientation of the coadsorbed solvent molecules. In the analysis of the images of the *S* enantiomer, only a positive angle is observed. In the model shown in Figure 2 A a few (*S*)-ISA molecules are presented together with the underlying graphite substrate. The absence of negative domains indicates that, as far as the packing of the (*S*)-ISA lamellae is concerned, the *S* enantiomer has formed an enantiomorphous monolayer.

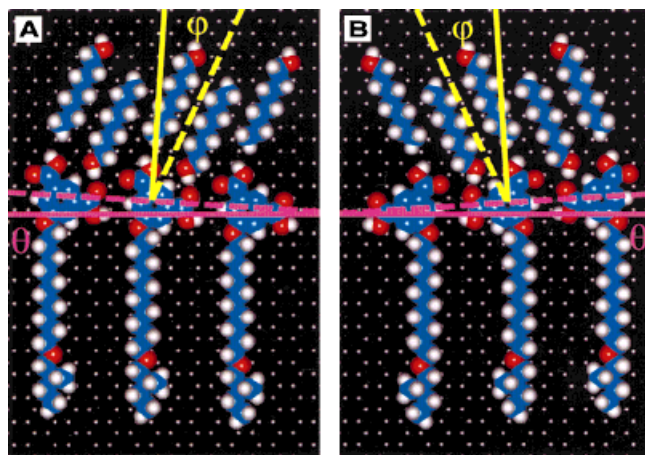


Figure 2. Proposed model for the molecular arrangement in A) a positive domain and B) a negative domain together with the underlying graphite substrate.  $\theta$  is the angle between the lamellar axis (purple dashed line) and the normal to that graphite axis which is in alignment with the alkoxy chains (purple solid line).  $\varphi$  is the angle between the solvent molecules (yellow dashed line) and the normal to the lamellar axis (yellow solid line).

(*R*)-ISA was also dissolved in 1-heptanol and applied to the graphite surface. Comparison of the monolayer structure with the underlying graphite surface reveals that the domains are negative ( $\theta = -3.8 \pm 0.6^\circ$ ). The STM image of (*R*)-ISA



presented in Figure 1D indicates that the alkoxy chains are interdigitated as for (*S*)-ISA. The intralamellar distance between two head groups is  $9.60 \pm 0.05$  Å. 1-Heptanol molecules are coadsorbed between adjacent lamellae of chiral molecules. The angle  $\varphi$  between the solvent molecules and an imaginary line perpendicular to a row of isophthalic head groups is  $-18 \pm 3^\circ$ . A proposed model for the monolayer in Figure 1D is shown in Figure 1E. In Figure 2B, a model is presented of a few (*R*)-ISA molecules together with the underlying graphite surface.

Leaving aside the packing of the solvent molecules, the only difference between positive domains (only found for (*S*)-ISA) and negative domains (only found for (*R*)-ISA) is the sign of the angle  $\theta$  between the lamellar axis and the normal to that graphite axis which is in alignment with the alkoxy chains. The lamellae built up by (*S*)-ISA or (*R*)-ISA molecules form positive or negative domains, respectively, which are enantiomorphous.

As already mentioned, in both positive and negative domains the coadsorbed 1-heptanol molecules are not oriented perpendicular to the lamellar axis of the isophthalic acid molecules. Moreover, the sign of the angle  $\varphi$  between the solvent molecules and the normal to the lamellar axis depends on the domain in which these molecules are coadsorbed. In all the STM images obtained, a positive value for  $\varphi$  is found in the positive domains formed by (*S*)-ISA molecules, and a negative angle is found in the negative domains formed by (*R*)-ISA molecules (presented schematically in Figure 2).<sup>[14]</sup> The absolute value of this angle varies from 7 up to  $25^\circ$ . This variation could find its origin in the difference in the relative position of the ISA head groups in two adjacent lamellae between which the solvent molecules are adsorbed, resulting in subtle differences in hydrogen bonding. As the solvent molecules will tend to optimize hydrogen bonding, they will adjust their orientation (angle) to obtain maximum stabilization.

Strictly spoken, positive and negative domains are not completely enantiomorphous, owing to the nonunique value for  $\varphi$ . It is therefore more appropriate to use the expression “quasi-enantiomorphous” in describing this system. However, the connection between the signs of  $\theta$  and  $\varphi$  makes it possible to unambiguously assign a domain as positive (consisting of *S* enantiomer) or negative (consisting of *R* enantiomer) without referring to the underlying graphite substrate. It is shown for the first time that the orientation of achiral coadsorbed molecules expresses the chirality of the domains.

In addition, STM images of the racemic mixture (*RS*)-ISA are obtained where a positive and a negative domain are observed in the same image (Figure 3). The inset of Figure 3 is a magnification of the domain boundary; the left domain is negative, the right domain positive. The two-dimensional packing of the isophthalic acid molecules within the positive and negative domains is identical to adlayers of (*S*)-ISA and (*R*)-ISA, respectively. This suggests that the racemic mixture forms a physisorbed monolayer composed of chiral, enriched, separated, quasi-enantiomorphous domains.

Control experiments on an achiral isophthalic acid derivative (5-octadecyloxyisophthalic acid) dissolved in 1-octanol showed that both positive and negative domains are formed.

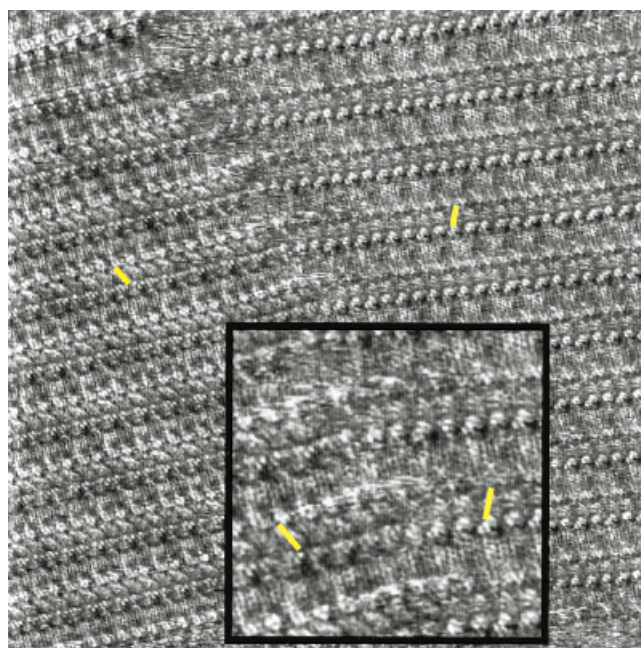


Figure 3. STM image of an ordered monolayer formed after applying a solution of the racemate (*RS*)-ISA on the graphite substrate; image size:  $37 \times 37$  nm<sup>2</sup>. The inset shows an enlargement of a part of the domain boundary ( $13.7 \times 13.7$  nm<sup>2</sup>). The left side of the image is a negative domain, and the right side a positive domain. The orientation of the coadsorbed solvent molecules, indicated by yellow lines, reflects the chirality of the respective domains.

The alcohol molecules did not reflect the chirality of the domains as both positive and negative values for  $\varphi$  are found, even within the same domain (image not shown). 5-[10-(Butoxy)decyloxy]isophthalic acid, the achiral analogue of the compound studied, is not an adequate reference compound as different monolayer structures were observed (image not shown).<sup>[15]</sup>

It can not only be concluded that molecular chirality is transferred to a chiral supramolecular packing mode, but also that achiral codeposited solvent molecules express the chirality of the monolayer.

### Experimental Section

(*R*)-, (*S*)-, and (*RS*)-ISA were prepared from the corresponding enantiomers or the racemate of 2-methyl-1-butanol. (*R*)-2-Methyl-1-butanol was obtained from (*R*)-2-methyl-1-butanoic acid<sup>[16]</sup> (*R*:*S*  $\approx$  92:8, determined by GC and the optical rotation) under retention of configuration as described in reference [17]. (*S*)-2-Methyl-1-butanol was purchased from Fluka (*S*:*R*  $\approx$  99:1, determined by GC). The enantiomeric ratios of (*R*)- and (*S*)-ISA were assumed to be identical with the ones of the corresponding starting alcohols, since no racemization could be detected in the course of the synthesis. Detailed preparation procedures and spectroscopic data will be reported elsewhere.

Prior to imaging, the compound was dissolved in 1-heptanol (Aldrich, 99%) at a concentration of approximately 5 mg mL<sup>-1</sup>. One drop of this solution was then applied to the basal plane of a piece of HOPG (grade ZYB, Advanced Ceramics Inc., Cleveland, OH). The tip was immersed in the solution and brought to the liquid/solid interface. The STM images were acquired in the variable-current mode (constant height) under ambient conditions. STM images obtained at low bias voltages reliably revealed the atomic structure of HOPG, providing an internal calibration standard for the monolayer studies. STM experiments were performed with a Discoverer scanning tunneling microscope (Topometrix Inc., Santa

Barbara, CA) along with an external pulse/function generator (Model HP 8111 A). Tips were electrochemically etched from Pt/Ir wire (80%/20%, diameter 0.2 mm) in an aqueous solution of 2N KOH and 6N NaCN. Typically, a tunneling current of 0.5–1 nA and a bias voltage of 0.2–1 V (sample negative) were employed. The STM images were corrected for instrumental drift.

Received: August 15, 1997 [Z 108231E]  
German version: *Angew. Chem.* **1998**, *110*, 1281–1284

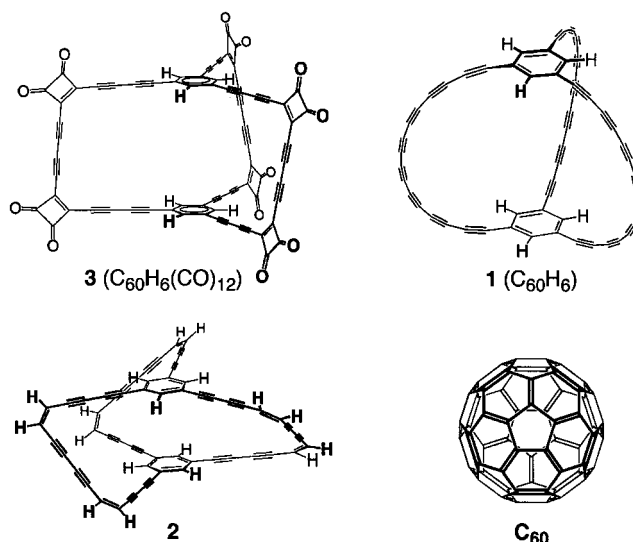
**Keywords:** chirality • monolayers • scanning tunneling microscopy

- [1] L. Pasteur, *C. R. Seances Acad. Sci.* **1848**, 26, 535–539.
- [2] G. Binnig, H. Rohrer, C. Gerber, E. Weibel, *Phys. Rev. Lett.* **1982**, *49*, 57–61.
- [3] G. Binnig, C. F. Quate, C. Gerber, *Phys. Rev. Lett.* **1986**, *56*, 930–933.
- [4] R. Viswanathan, J. A. Zasadzinski, D. K. Schwarz, *Nature* **1994**, *368*, 440–443.
- [5] D. P. E. Smith, *J. Vac. Sci. Technol. B* **1991**, *9*, 1119–1125.
- [6] S. J. Sowerby, W. M. Heckl, G. B. Petersen, *J. Mol. Evol.* **1996**, *43*, 419–424.
- [7] J. P. Rabe, S. Buchholz, *Phys. Rev. Lett.* **1991**, *66*, 2096–2099.
- [8] C. J. Eckhardt, N. M. Peachy, D. R. Swanson, J. M. Takacs, M. A. Khan, X. Gong, J.-H. Kim, J. Wang, R. A. Uphaus, *Nature* **1993**, *362*, 614–616.
- [9] a) F. Stevens, D. J. Dyer, D. M. Walba, *Angew. Chem.* **1996**, *108*, 955–957; *Angew. Chem. Int. Ed. Engl.* **1996**, *35*, 900–901; b) D. M. Walba, F. Stevens, N. A. Clark, D. C. Parks, *Acc. Chem. Res.* **1996**, *29*, 591–597.
- [10] a) P. Nassoy, M. Goldman, O. Bouloussa, F. Rondelez, *Phys. Rev. Lett.* **1995**, *75*, 457–460. b) I. Weissbuch, M. Berfeld, W. Bouman, K. Kjaer, J. Als-Nielsen, M. Lahav, L. Leisorowitz, *J. Am. Chem. Soc.* **1997**, *119*, 933–942.
- [11] P. Vanoppen, P. C. M. Grim, M. Rücker, S. De Feyter, G. Moessner, S. Valiyaveetil, K. Müllen, F. C. De Schryver, *J. Phys. Chem.* **1996**, *100*, 19636–19641.
- [12] P. C. M. Grim, S. De Feyter, A. Gesquière, P. Vanoppen, M. Rücker, S. Valiyaveetil, G. Moessner, K. Müllen, F. C. De Schryver, *Angew. Chem.* **1997**, *109*, 2713–2715; *Angew. Chem. Int. Ed. Engl.* **1997**, *36*, 2601–2603.
- [13] Positive is defined as going clockwise from the normal towards the orientation of the organized structure. The normal can be related to the graphite axis ( $\theta$ ) or the lamellar axis ( $\varphi$ ; Figure 2).
- [14] Our conclusions are based upon approximately 50 STM images for each enantiomer. None of the STM images obtained are in contradiction with the results outlined in the text.
- [15] This compound forms two types of monolayer structures. Some domains are completely disordered and contain ringlike structures, individual small lamellae, etc. Other domains are composed of lamellae, but the lamellar width ( $20 \pm 1$  Å) and the intralamellar distance between two head groups ( $8.4 \pm 0.2$  Å) are much smaller than the values obtained for ISA molecules. The angle between the alkoxy chains and the lamellar axis measures approximately  $43 \pm 2^\circ$ . No codeposition of solvent molecules was observed. These large deviations are most likely due to the presence of an ether functionality in the alkyl chain and the absence of a stereogenic center. In ISA these stereogenic centers force, probably because of sterical hindrance, the side chains to adapt an extended conformation that is almost perpendicular to the lamellar axis.
- [16] K. Freudenberg, W. Lwowski, *Justus Liebigs Ann. Chem.* **1955**, *594*, 76–88.
- [17] M. Hjalmarsson, H.-E. Högborg, *Acta Chem. Scand. Ser. B* **1985**, *39*, 793–796.

## Acetylenic Cyclophanes as Fullerene Precursors: Formation of $C_{60}H_6$ and $C_{60}$ by Laser Desorption Mass Spectrometry of $C_{60}H_6(CO)_{12}$ \*\*

Yves Rubin,\* Timothy C. Parker, Salvador J. Pastor, Satish Jalasatgi, Christophe Boulle, and Charles L. Wilkins\*

In previous reports<sup>[1]</sup> we proposed that highly unsaturated macrocyclic cyclophanes such as **1** and **2** may function as precursors of the fullerene  $C_{60}$  and its endohedral metal complexes in a process analogous to the coalescence annealing of mono- and polycycles with *sp*-hybridized carbon atoms during the gas-phase formation of fullerenes from evaporated graphite (Scheme 1).<sup>[2, 3]</sup> Formation of endohedral transition metal complexes by this route is particularly appealing in view of the exceptional physical and chemical properties of  $C_{60}$ .<sup>[4]</sup> Here we report for the first time that the acetylenic macrocycle **3** effectively leads to  $C_{60}H_6$  and  $C_{60}$  ions in the gas phase in laser desorption mass spectroscopic experiments.<sup>[5]</sup>



Scheme 1. Structures of the acetylenic macrocycles **1–3** and of  $I_h-C_{60}$ .

When the thermochemistry of macrocycle **2** was studied by matrix assisted laser desorption ionization Fourier transform (MALDI-FT) and atmospheric pressure chemical ionization

[\*] Prof. Y. Rubin, Dr. T. C. Parker, Dr. S. Jalasatgi, Dr. C. Boulle  
Department of Chemistry and Biochemistry  
University of California, Los Angeles  
Los Angeles, CA 90095-1569 (USA)  
Fax: (+1) 310-206-7649  
E-mail: rubin@chem.ucla.edu  
Prof. C. L. Wilkins, S. J. Pastor  
Department of Chemistry  
University of California, Riverside  
Riverside, CA 92521 (USA)  
Fax: (+1) 909-787-4713  
E-mail: cwilkins@citrus.ucr.edu

[\*\*] We are grateful to the Office of Naval Research (N00014-94-1-0534, Y.R.) and the NIH (grant GM44606, C.L.W.) for financial support.